

Simultaneous memory effects in the stress and in the dielectric susceptibility of a stretched polymer glass

J. Hem¹, C. Crauste-Thibierge¹, F. Clément², D.R. Long², S. Ciliberto¹,

¹ *Univ of Lyon, Ens de Lyon, Univ Claude Bernard, CNRS,
Laboratoire de Physique, UMR 5672, F-69342 Lyon, France and*

² *Laboratoire Polymères et Matériaux Avancés, CNRS/Solvay, UMR 5268, 69192 Saint Fons Cedex, France*

We report experimental evidence that a polymer stretched at constant strain rate $\dot{\gamma}$ presents complex memory effects after that $\dot{\gamma}$ is set to zero at a specific strain λ_w for a duration t_w , ranging from 100s to 2.2×10^5 s. When the strain rate is resumed, both the stress and the dielectric constant relax to the unperturbed state non monotonically. The relaxations depend on the observable, on λ_w and on t_w . Relaxation master curves are obtained by scaling the relaxation time as $t/\ln(t_w)$. The dielectric evolution also captures the distribution of the relaxation times, so the results impose strong constraints on the relaxation models of polymers under stress and they can be useful for a better understanding of memory effects in other disorder materials.

Aging of amorphous and heterogeneous materials is characterized by a slow relaxation toward a new state after that a perturbation has been applied [1]. This relaxation usually spans several orders of magnitude in time and most importantly may present memory effects, which depend on the sample history (see Ref. [2] for a recent review).

Memory effects are ubiquitous of aging and they have been observed in glassy and disordered materials [3–11], and also in many other disordered systems [12–19]. Memory effects may take the form of a Kovacs-like nonmonotonic relaxation. This is a surprising and non intuitive phenomenon because with no external input after the initial driving, a state variable evolves in one direction before turning around after some timescale that was imprinted during the prior driving history. Such relaxations have been observed in the mechanical [6] and electrical [7] responses of polymer glasses, in the static coefficient of friction [12, 13], the load on crumpled thin sheets [14, 15] and the mechanical response of granular systems [17–19].

Several theoretical models [10, 20–24] have been developed to explain, with common underlying physical principles, the similar features of these complex relaxations observed in very different systems. One of the key assumptions of these models is the existence into these disordered systems of a distribution of relaxation times (DRT) which is used to explain the origin of aging and of non-monotonic relaxations. However it is hard to discern between the different descriptions using experiments in which only one observable is measured. Thus to give more insight into this problem, we performed more complex experiments where one gets quantitative information on the memory of several observables measured simultaneously and on the evolution of the DRT.

In this letter we describe these experiments and we report the observation that a stretched polymer glass exhibits complex memory effects of the stress and of the dielectric susceptibility. Specifically, we show that, after a perturbation of the strain rate, the relaxation dynamics of the stress and the dielectric susceptibility present

non monotonic responses which depend not only on the sample history, as in the above mentioned Kovacs-like memory effect, but also on the observable. Furthermore from the evolution of the dielectric spectra we get insights on the evolution of the polymer DRT. Thus our results impose constraints for modeling the dynamic processes of two interrelated quantities and the polymer relaxation dynamics under deformation, which is widely studied, both experimentally [25–30] and theoretically [31–35].

In our experiment the investigated polymer is an extruded film MAKROFOL DE[®] 1-1 000000 from BAYER based on Makrolon[®] polycarbonate (PC) of thickness 125 μm . The films are cut into rectangular pieces of size $42 \times 21\text{cm}$ with a dog bone shape before being tied to the tensile machine. During the experiment, we measure the instantaneous stress $\sigma(t)$ and deformation $\lambda(t) = L(t)/L_0$ of the films. The experiment are performed at $T = 25^\circ\text{C}$ much below the glass transition temperature $T_g = 150^\circ\text{C}$. In parallel to the stress measurement we use the dielectric spectroscopy to investigate the dynamics of the relaxation processes at work in the film. For the dielectric measure, two electrodes sandwich the film in contact by an aqueous gel and are connected to an homemade dielectric spectrometer spanning simultaneously 5 decades in frequency (10^{-2}Hz to 10^3Hz) (more details about the experimental apparatus can be found in Ref. [29, 30, 36]). Dielectric spectroscopy is a convenient way to probe in-situ and without destruction the relaxation times of stretched polymers [29, 30, 37]. It is worth to mention that other techniques, such as NMR measurements [25] or probe molecule experiments [26, 27], can be used but dielectric spectroscopy is very versatile. In the rest of the paper, we will focus only on the loss tangent $\tan\delta(f) = -\epsilon''(f)/\epsilon'(f)$, which does not depend on the film thickness, being the ratio of the imaginary (ϵ'') and real (ϵ') parts of the dielectric susceptibility, measured at frequency f .

We first recall the behavior of the stress and the dielectric susceptibility as a function of λ measured at constant strain rate $\dot{\gamma}$, that we have extensively discussed

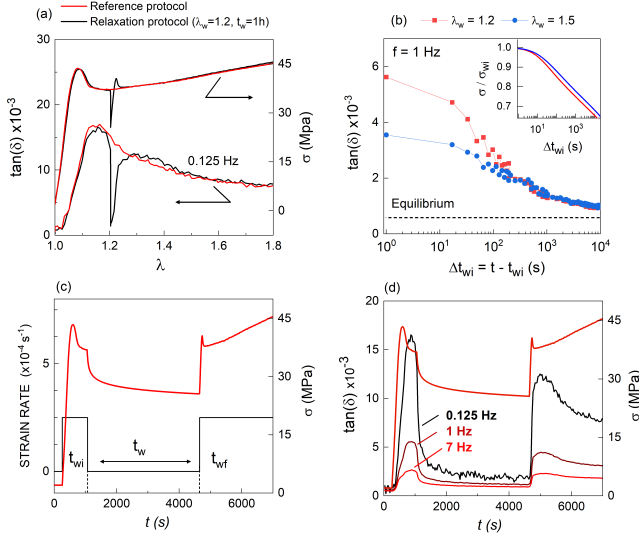


FIG. 1. (a) Dielectric susceptibility $\tan\delta$ at $f = 0.125 Hz$ and stress σ as function of the strain λ . Evolutions under constant strain rate $\dot{\gamma} = 2.5 \times 10^{-4} s^{-1}$ in black, called reference curves. Evolutions under the relaxation protocol $\lambda_w = 1.2$ and $t_w = 1h$ in red. (b) Temporal evolutions of $\tan\delta$ at $f = 1 Hz$ and the normalized stress σ/σ_w (inset) during the waiting step over $t_w = 10h$. (c) $\dot{\gamma}(t)$ and $\sigma(t)$ during the entire relaxation protocol with $\lambda_w = 1.2$, $t_w = t_{wf} - t_{wi} = 1h$. Times t_{wi} and t_{wf} delimit the beginning and the end of the waiting interval respectively. (d) $\sigma(t)$ and $\tan\delta(t)$ at $f = 0.125, 1, 7 Hz$.

in Ref. [29, 30]. Fig.1(a) depicts the stress evolution for polycarbonate at $\dot{\gamma} = 2.5 \times 10^{-4} s^{-1}$ (black curve). The stress first increases until the yield stress at about $\lambda = 1.08$, then, successively decreases, a regime known as strain softening, reaches a plateau at about $\lambda = 1.20$ and finally increases again, which is known as strain hardening. The breaking occurs at about $\lambda = 1.8 - 2$. In parallel to the stress measurement we have probed the local dynamic of stretched polymer using dielectric spectroscopy in the range $10^{-2} Hz$ to $10^3 Hz$. As described in Ref. [29, 30, 37], dielectric measurements give access to the evolution of the dominant relaxation time τ_α of the polymer by identifying the lower part of the dielectric spectrum ($10^{-2} Hz$ to $10^0 Hz$) as the high frequency tail of the α relaxation peak. In particular, we have shown in ref. [30] that the increase (decrease) of the dielectric susceptibility in the range $10^{-2} Hz$ to $10^0 Hz$ reflects a decrease (increase) of τ_α , which depends on λ and the strain rate $\dot{\gamma}$. Therefore, the evolution of $\tan\delta$ at $f = 0.125 Hz$ depicted in Fig.1(a) shows an acceleration of the relaxation times until the softening/onset of plastic flow (maximum around $\lambda = 1.15 - 1.17$) and a slow down during the strain hardening regime that we have studied in Ref. [30]. Notice that, at $\dot{\gamma}$ constant, $\tan\delta$ and σ have a similar behavior as a function of λ up to the onset of the strain hardening regime. The results of the measurements performed at constant $\dot{\gamma}$ (black curves in Fig.1(a)) will be

called "reference curves".

To investigate the memory effect, we have modified the protocol at constant $\dot{\gamma}$ in order to include an aging step at a specific λ in the post yield regime of the film. More precisely, the film is first stretched at $\dot{\gamma} = 2.5 \times 10^{-4} s^{-1}$ then held at the waiting strain λ_w during the waiting time t_w , and finally further stretched with the same initial $\dot{\gamma}$. As an example for the case $\lambda_w = 1.2$ (strain softening) and $t_w = 1h$, the evolutions of σ and of $\tan\delta(0.125)$ are illustrated as a function of λ in Fig.1(a). The corresponding time evolution is illustrated in Figs.1(c),1(d) where the instantaneous strain rate $\dot{\gamma}$ is indicated too. Three different intervals can be distinguished: During the initial one ($\lambda < \lambda_w$ and $t < t_{wi}$), σ and $\tan\delta$ are identical to the reference curves, see Fig.1(a). During the waiting interval (i.e. $\lambda_w = 1.2$ and $t_{wi} \leq t \leq t_{wf}$), they decrease logarithmically with time, which is the signature of an aging process, see Fig.1(b). Finally as soon as $\dot{\gamma}$ is resumed for $t \geq t_{wf}$, they increase again but faster than at the beginning of the experiment. In Fig.1(a), the comparison with the reference curves obtained with the constant strain rate protocol shows that σ and $\tan\delta(0.125)$ finally recover their reference curves. However notice that, in spite of the fact that σ and $\tan\delta(0.125)$ have a similar dependence on λ before the aging step, the recoveries of the two observables are rather different, see Figs.1(a),1(d). In addition, we shall see that these recovery processes also depend on t_w and on λ_w .

Before presenting these results, we want to point out that Fig.1(d) shows that the response of $\tan\delta$ to $\dot{\gamma}$ increases by reducing the frequency f . From this frequency dependence we get useful information on the DRT evolution by studying the whole spectrum of $\tan\delta$. Thus we plot the $\tan\delta$ spectra in Fig.2(a) during the waiting interval at $\lambda_w = 1.2$ and in Fig.2(b) during the recovery for $t > t_w = 1h$. We first notice that the spectra evolve in a significant way only for $f < 100 Hz$. Furthermore, we see in Fig.2(a) that the spectrum at $\lambda = 1.2$, at the beginning of the aging ($t = t_{wi}$), is identical to the reference one obtained during the constant $\dot{\gamma}$ protocol. Then, during the waiting interval for increasing $\Delta t_{wi} = t - t_{wi}$, the spectrum progressively decreases towards the equilibrium spectrum (i.e. the spectrum at $\lambda = 1$). Inversely, in Fig.2(b), the spectra during the recovery interval increase again until they reach the reference spectrum around $\lambda = 1.3$, i.e. $\Delta t = t - t_{wf} = 400s$.

The main relaxation time can be estimated from these spectra following the method presented in Ref.[30] in which we have shown that at low frequencies $\tan\delta(f) \simeq (\sin \beta\pi/2)/(2\pi f \tau_{eff})^\beta$ where the characteristic time τ_{eff} and the exponent β have to be determined. Within the Cole-Cole [38] model, τ_{eff} is proportional to the main relaxation time τ_α of the polymer and the exponent β is related to the width of the distribution of the relaxation times, specifically the smallest is $\beta < 1$ the larger is the

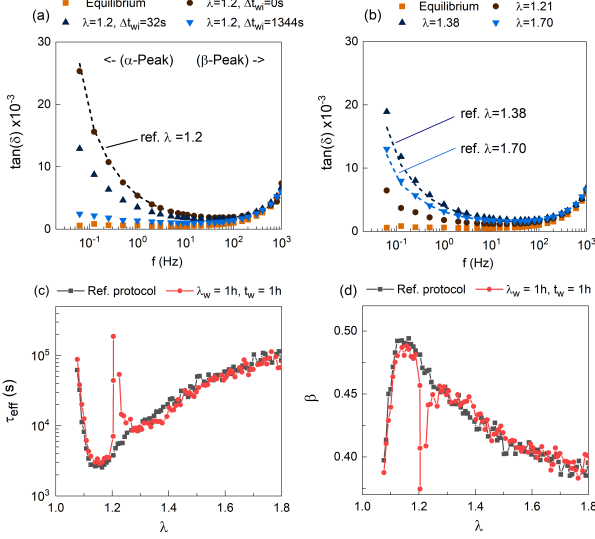


FIG. 2. Dielectric spectra $\tan\delta$ recorded at different times for the relaxation protocol at $\lambda_w = 1.2$ and $t_w = 1h$. Evolution during the aging interval at $\lambda = 1.2$ with $\Delta t_{wi} = t - t_{wi}$ (a) and during the recovery interval for $\lambda > 1.2$ (b). Dashed lines correspond to the reference spectra recorded at constant $\dot{\gamma}$. The evolutions of τ_{eff} and β are plotted in (c) and (d) respectively. Red lines correspond to the relaxation protocol and black lines to the reference at constant $\dot{\gamma}$.

distribution [28, 30]. Thus the fit of the low frequencies part of the spectra in Figs.2(a),2(b) (recorded at different times) allows us to estimate the evolution of the DRT during the relaxation protocol. In particular, we see in Figs.2(c),2(d) that, during the waiting interval, τ_{eff} (β) increases (decreases), meaning that not only the dynamics slow down but that the distribution of times is broadening. When the strain rate is resumed the dynamics accelerate again and the distribution shrinks, recovering the reference state after the resumption. Hence, this is the evidence that the DRT depends on the driving history and that $\dot{\gamma}$ accelerates the polymer dynamics, even if the acceleration is not monotonous in λ .

To study the evolution of $\tan\delta$ as a function of t_w and λ_w , we now select $\tan\delta$ measured at $f = 0.125\text{Hz}$ as a typical amplitude of the low frequency spectra, which depend on τ_α and β . Figs.3(a-d) bring more details on the recovery processes by showing different results of tests performed with different waiting times and waiting strains $\lambda_w = 1.2$ (strain softening) in Figs.3(a),3(c) and $\lambda_w = 1.5$ (strain hardening) in Figs.3(b),3(d). When $\dot{\gamma}$ is resumed at t_{wf} , we observe that the relaxations of the stress σ and the dielectric susceptibility $\tan\delta$ are both non-monotonic and exhibit an overshoot above the reference curve before relaxing to it, with different shapes of the evolutions of the two observables. On one side, the stress overshoot has a distinct and large amplitude while occurring rapidly after the resumption, see Figs.3(a),3(b). In contrast, the

overshoot of the dielectric constant has a weaker amplitude and occurs much later in time, see Figs.3(c),3(d).

Moreover, we find that the waiting time has a strong impact on the relaxation. In the case of the stress, Figs.3(a),3(b) show that, as long as t_w increases, the overshoot peak shifts progressively to longer time and presents a higher and sharper amplitude. In the case of the dielectric susceptibility, Figs.3(c),3(d) show that an increase of t_w also shifts the peak time and slows down the relaxation to the reference curve. Also in the dielectric case, we observe that a longer t_w affect the peak amplitude.

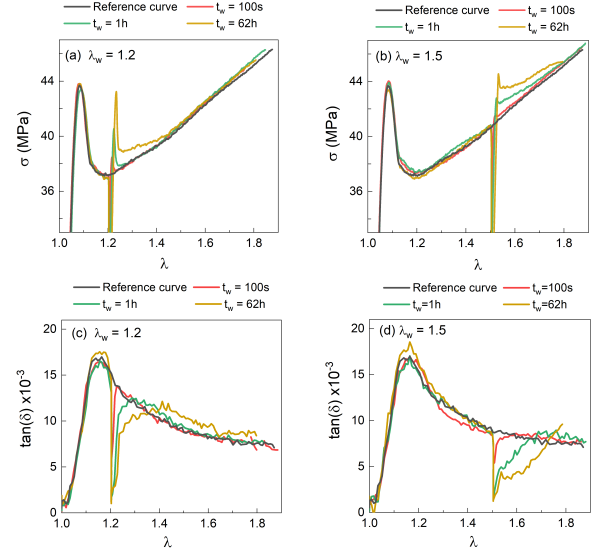


FIG. 3. Stress σ and dielectric susceptibility $\tan\delta$ at $f = 0.125\text{Hz}$ as a function of λ for different λ_w and t_w . Curves obtained by averaging at least three tests. (a,c) σ and $\tan\delta$ at $\lambda_w = 1.2$ (in the strain softening). (b,d) σ and $\tan\delta$ at $\lambda_w = 1.5$ (in the strain hardening). The reference curves are indicated in black. Note the stress axis have been expanded in (a,b) with respect to Fig.1a).

Besides the waiting time, the choice of the waiting strain also modifies the relaxation. Figs.3(a),3(b) show qualitatively that the overshoot peak is higher and narrower at $\lambda_w = 1.2$ than at $\lambda_w = 1.5$ and at the same time Figs.3(c),3(d) show that $\tan\delta$ recovers much faster the reference curve at $\lambda_w = 1.2$ than at $\lambda_w = 1.5$. The difference is significant. For example at $t_w = 1h$ and $\lambda_w = 1.2$, $\tan\delta$ recovers the reference curve at about $\lambda = 1.45$, equivalent to $\Delta t = t - t_{wf} = 1024s$ after the resumption of the stretching. This is much faster than for the case at $t_w = 1h$ and $\lambda_w = 1.5$ for which the recovery is even too long to occur during our experiment ($\lambda > 1.85$ equivalent to $\Delta t > 1240s$). Since the relaxation of the observables are affected by the waiting time t_w at fixed waiting strain λ_w and reciprocally by λ_w at fixed t_w , one must conclude that these two aging parameters λ_w and t_w govern independently the relaxation during the recovery process.

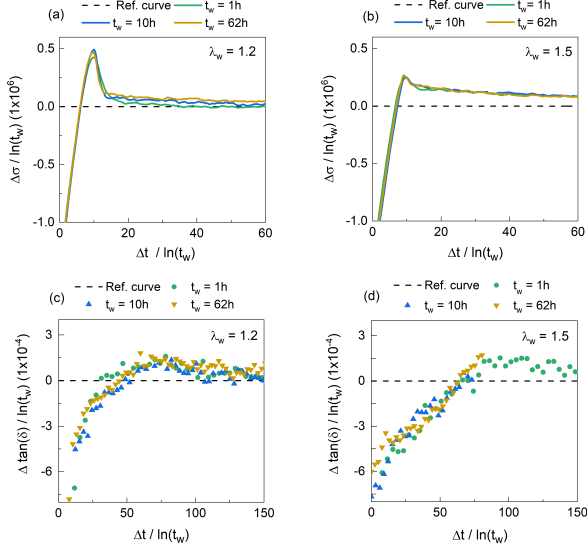


FIG. 4. (a,b) Evolution of $\Delta\sigma/\ln(t_w)$ as function of $\Delta t/\ln(t_w)$ with $\Delta\sigma = \sigma - \sigma_{ref}$ and $\Delta t = t - t_{wf}$ during the recovery step, (a) at $\lambda_w = 1.2$ and (b) at $\lambda_w = 1.5$. (c,d) Dependence of $\Delta \tan\delta/\ln(t_w)$ as function of $\Delta t/\ln(t_w)$ with $\Delta \tan\delta = \tan\delta - \tan\delta_{ref}$ during the recovery step, (c) at $\lambda_w = 1.2$ and (d) at $\lambda_w = 1.5$.

To be more precise regarding the dependence of the relaxations on those aging parameters we analyze the difference between the stress curve and the reference one $\Delta\sigma = \sigma - \sigma_{ref}$ as a function of the time $\Delta t = t - t_{wf}$ elapsed after resumption. Figs.4(a),4(b) show that all the relaxation curves, measured after different waiting times t_w , can be superimposed by scaling $\Delta\sigma$ and Δt by the logarithm of t_w , for $t_w > 100$ s. Moreover, we observe that this relation holds regardless of the waiting strain value ($\lambda_w = 1.2$ or $\lambda_w = 1.5$). As a consequence, this means that the peak time and the peak amplitude depend on $\ln(t_w)$. Regarding the dependence of the peak properties on t_w and λ_w , we note, that the peak amplitude $\Delta\sigma_p$ is different for the two waiting strains, being higher at $\lambda_w = 1.2$ than at $\lambda_w = 1.5$ for all t_w . In contrast the peak time Δt_p is independent on the waiting strain, see Fig.4(a),4(b).

Finally, it is interesting to see that this way of scaling the data also works for the dielectric susceptibility. In a similar way than before, we have studied the evolution of the difference between the $\tan\delta$ curve at $f = 0.125\text{Hz}$ and the reference one $\Delta \tan\delta = \tan\delta - \tan\delta_{ref}$ as function of Δt . Figs.4(c),4(d) show that all the relaxation curves merge together by rescaling $\Delta \tan\delta$ and Δt by $\ln(t_w)$. This is observed again for the two waiting strains investigated, either at $\lambda_w = 1.2$ (Fig.4(c)) or at $\lambda_w = 1.5$ (Fig.4(d)). Note that for the dielectric case, the peak time at $\lambda_w = 1.5$ is delayed compared to $\lambda_w = 1.2$ which was not the case for the stress relaxation. The logarithmic dependence on t_w shows, in particular, that the

memory of the aging history can also occur in $\tan\delta$, so that we provide evidence that the memory appears simultaneously in different observables but in different ways.

Concerning the scaling $\Delta t/\log(t_w)$, we point out that in several systems with non-monotonous relaxations, the memory effects present a $\Delta t/t_w$ scaling [2, 15, 22], which however is not generic. In several cases [4], a heuristic form of scaling $\Delta t/t_w^\mu$ is used, which has been theoretically justified [21]. If $\mu < 1$ then $\log t_w$ cannot be distinguished from t_w^μ , and our scaling $\Delta t/\log(t_w)$ can be understood within this theoretical framework. In these models the DRT does not depend on time whereas our measurements show that it does evolve, thus our measure of the DRT evolution will help in constructing more precise models. It remains to understand why the time scale of the relaxations are different for σ and $\tan\delta$. It is interesting to notice that for polymers the amplitude of the main yield stress peak also undergoes a similar logarithmic dependence on the aging time \tilde{t}_w , which in this case is the time spent in the glassy state after a temperature quench from the melt [39–42]. However in contrast to our experiment the positions of the yield peak does not depend on \tilde{t}_w . This difference could be related to the way the waiting step is realized. Indeed when the polymer ages after a temperature quench no stress is applied to the sample before the measure of the loading curve, whereas in our experiment the polymer ages from the plastic regime at constant strain. From this perspective, it must be concluded that stretching affects substantially the aging and the recovery processes, which is confirmed by the dependence of the memory effects on λ observed in our experiment. The evolution of the dielectric susceptibility and of the DRT when a stress is applied after the time \tilde{t}_w has never been measured, and no comparison with our results can be done. This comparison would be very useful for giving new insights to the polymer relaxations under stress.

As a conclusion, we have shown that a stretched polymer presents complex memory effects of the σ and of the $\tan\delta$ relaxations. The measure of $\tan\delta$ as a function of frequency allows us to have information on the evolution of the DRT. Thus our results, by showing important features of the dynamical processes of two interrelated quantities and of the polymer relaxation dynamics, challenge the theoretical models of the memory effect in glassy materials and disordered systems.

J. Hem acknowledges the funding by Solvay. We thank O.Razebassia for helpful assistance on the tensile machine and the Bartolo team for lending the cutting plotter.

- [2] N. C. Keim, J. D. Paulsen, Z. Zeravcic, S. Sastry, and S. R. Nagel, *Rev. Mod. Phys.* **91**, 035002 (2019).
- [3] V. Dupuis, F. Bert, J. Bouchaud, J. Hamman, F. Ladieu, D. Parker, and E. Vincent, *Pramana* **64**, 1109 (2005).
- [4] E. Vincent, *Lecture Notes in Physics* **716**, 7 (2007).
- [5] H.E. Castillo, C. Chamon, L. Cugliandolo, and M.P. Kennett, *Phys. Rev. Lett.* **88** (2002), 10.1103/PhysRevLett.88.237201.
- [6] A. J. Kovacs, *Adv. Polym. Sci.*, 394 (1963).
- [7] A. Alegria, L. Goitiandia, I. Telleria, and J. Colmenero, *Macromolecules* **30**, 3881 (1997).
- [8] L. Bellon, S. Ciliberto, and C. Laroche, *Eur. Phys. Lett.*, 551 (2000).
- [9] L. Bellon, S. Ciliberto, and C. Laroche, *Eur. Phys. J. B* **25**, 223 (2002).
- [10] A. Amir, S. Borini, Y. Oreg, and Y. Imry, *Phys. Rev. Lett.* **107**, 186407 (2011).
- [11] T. Divoux, V. Grenard, and S. Manneville, *Phys. Rev. Lett.* **110**, 018304 (2013).
- [12] S. M. Rubinstein, G. Cohen, and J. Fineberg, *Phys. Rev. Lett.* **96**, 256103 (2006).
- [13] S. Dillavou and S. M. Rubinstein, *Phys. Rev. Lett.* **120**, 224101 (2018).
- [14] K. Matan, R. B. Williams, T. A. Witten, and S. R. Nagel, *Phys. Rev. Lett.* **88**, 076101 (2002).
- [15] Y. Lahini, O. Gottesman, A. Amir, and S. M. Rubinstein, *Phys. Rev. Lett.* **118**, 085501 (2017).
- [16] J.B. Knight, C. G. Fandrich, C.N. Lau, H.N. Jaeger, and S.R. Nagel, *Phys. Rev. E* **51**, 3957 (1995).
- [17] A. Prados and E. Trizac, *Phys. Rev. Lett.* **112**, 198001 (2014).
- [18] C. Josserand, A. V. Tkachenko, D. M. Mueth, and H. M. Jaeger, *Phys. Rev. Lett.* **85**, 3632 (2000).
- [19] K. A. Murphy, J. W. Kruppe, and H. M. Jaeger, *Phys. Rev. Lett.* **124**, 168002g (2020).
- [20] E. Bertin, J. Bouchaud, J. Drouffe, and C. Godreche, *J. Phys. A* **36**, 10701 (2003).
- [21] P. Sibani and G. G. Kenning, *Phys. Rev. E* **81**, 011108 (2010).
- [22] A. Amir, Y. Oreg, and Y. Imry, *Proc. Natl. Acad. Sci. U.S.A.* **109**, 1850 (2012).
- [23] S. Merabia and D. Long, *J. Chem. Phys.* **125**, 234901 (2006).
- [24] D. R. Long, L. Conca, and P. Sotta, *Phys. Rev. Mater.* **2**, 105601 (2018).
- [25] L. S. Loo, R. E. Cohen, and K. K. Gleason, *Science* **288**, 116 (2000).
- [26] H.-N. Lee, K. Paeng, S. F. Swallen, and M. D. Ediger, *J. Chem. Phys.* **128**, 134902 (2008).
- [27] H.-N. Lee, K. Paeng, S. F. Swallen, and M. D. Ediger, *Science* **323**, 231 (2009).
- [28] H.-N. Lee and M. D. Ediger, *Macromolecules* **43**, 5863 (2010).
- [29] R. Perez-Aparicio, D. Cottinet, C. Crauste-Thibierge, L. Vanel, P. Sotta, J.-Y. Delannoy, D. R. Long, and S. Ciliberto, *Macromolecules* **49**, 3889 (2016).
- [30] R. Sahl, J. Hem, C. Crauste-Thibierge, F. Clement, D. R. Long, and S. Ciliberto, *Phys. Rev. Mater.* **4**, 035601 (2020).
- [31] R. S. Hoy and M. O. Robbins, *Polymer Physics* **47**, 1406 (2009).
- [32] K. S. Schweizer and E. J. Saltzman, *J. Chem. Phys.* **121**, 1984 (2004).
- [33] K. Chen and K. S. Schweizer, *Phys. Rev. Lett.* **102**, 038301 (2009).
- [34] L. Conca, A. Dequidt, P. Sotta, and D. R. Long, *Macromolecules* **50**, 9456 (2017).
- [35] R. A. Riggleman, H.-N. Lee, M. D. Ediger, and J. J. de Pablo, *Phys. Rev. Lett.* **99**, 215501 (2007).
- [36] R. Pérez-Aparicio, C. Crauste-Thibierge, D. Cottinet, M. Tanase, P. Metz, L. Bellon, A. Naert, and S. Ciliberto, *Rev. Sci. Instrum.* **86**, 044702 (2015).
- [37] J. Kalfus, A. Detwiler, and A. J. Lesser, *Macromolecules* **45**, 4839 (2012).
- [38] S. Havriliak and S. Negami, *J. Polym. Sci. Part C-Polymer Symposium*, 99 (1966).
- [39] C. Bauwens-Crowet and J. C. Bauwens, *Polymer* **23**, 1599 (1982).
- [40] H. E. H. Meijer and L. E. Govaert, *Prog. Polym. Sci.* **30**, 915 (2005).
- [41] E. T. J. Klompen, T. A. P. Engels, L. E. Govaert, and H. E. H. Meijer, *Macromolecules* **38**, 6997 (2005).
- [42] C. B. Roth, ed., *Polymer Glasses* (CRC Press, Boca Raton, 2017).